Turkish Journal of Engineering & Environmental Sciences

http://journals.tubitak.gov.tr/engineering/

Research Article

Turkish J Eng Env Sci
(2014) 38: 434 – 454

doi:10.3906/muh-1401-14

Hall effects on hydromagnetic free convection in a heated vertical channel in the presence of an inclined magnetic field and thermal radiation

Sankar Kumer GUCHHAIT[1], **Rabindra Nath JANA**[1], **Sanatan DAS**[2,*]
[1]Department of Applied Mathematics, Vidyasagar University, Midnapore, India
[2]Department of Mathematics, University of Gour Banga, Malda, India

Received: 22.01.2014 • **Accepted/Published Online:** 29.12.2015 • **Printed:** 04.03.2016

Abstract: An analytical study on unsteady hydromagnetic free convective flow of a viscous incompressible electrically conducting fluid in the presence of an inclined magnetic field taking Hall currents into account has been presented. The governing equations are solved analytically using the Laplace transform technique. The variations of the fluid velocity components and the fluid temperature are shown graphically and are discussed. The shear stresses and the rate of heat transfer at the channel plates are derived. The results are shown in figures and tables followed by a quantitative discussion.

Key words: Hydromagnetic, free convection, Hall currents, thermal radiation

1. Introduction

Hydromagnetic fluid dynamics continue to attract the attention of the applied mathematics and engineering sciences communities owing to considerable practical applications of such flows in plasma aerodynamics [1], magnetohydrodynamic (MHD) energy systems [2], nuclear engineering control [3], astrophysical fluid dynamics [4], and mechanical engineering manufacturing processes [5,6]. Often such flows may occur from very low Reynolds numbers to high-speed supersonic flows and also simultaneously with electromagnetofluid dynamic effects (Hall currents, ion slip, Alfven waves, etc.) and thermophysical phenomena, which can exert a substantial influence on velocity evolution and in the case of induction problems and magnetic field distributions. MHD convection flow has many important engineering applications in the design of power generators, heat exchangers, pumps, and flow meters; in solving space vehicle propulsion, control, and reentry problems; in designing communications and radar systems; in creating novel power-generating systems; in developing confinement schemes for controlled fusion; and in the design of nuclear cooling reactors and MHD accelerators.

Due to the varied range of applications in engineering and the universe, MHD free convection flow has become significant. A fluid flow in which the motion is a result of body force acting on the fluid in which there are density gradients is called a free convection flow. Temperature or concentration gradients existing in the fluid yield density gradients while the gravitational force yields the body force. Thus, the action of the body force on the fluid amounts to a buoyancy force that eventually induces free convection current. The radiative convective flows are frequently encountered in many scientific and environmental processes such as astrophysical flows, water evaporation from open reservoirs, heating and cooling of chambers, and solar power technology. Heat transfer by simultaneous radiation and convection has applications in numerous technological problems

*Correspondence: tutusanasd@yahoo.co.in

including combustion, furnace design, nuclear reactor safety, fluidized bed heat exchanger, fire spreads, solar fans, solar collectors, natural convection in cavities, turbid water bodies, photochemical reactors, and many others. The free convection in channels formed by vertical plates has received attention among researchers in the last few decades due to its widespread importance in engineering applications like cooling of electronic equipment, design of passive solar systems for energy conversion, design of heat exchangers, human comfort in buildings, thermal regulation processes, and many more.

Hall effects are important when the magnetic field is high or when the collision frequency is low (see [7]). The current induced in a fluid is usually carried predominantly by electrons, which are considerably more mobile than ions. The electron drift velocity in most cases leads to a second component of the flow velocity, which in turn leads to a secondary force and causes anisotropic electrical conductivity in the flow. The current component created by this anisotropic conductivity is known as the Hall current. The dimensionless product $\omega_e\tau_e$, usually called the Hall parameter, is an important characteristic number in the MHD design, where ω_e is the electron cyclotron frequency and τ_e is the electron collision mean free time. On the microscopic scale, the Hall parameter indicates the average angular travel of electrons between collisions, while on the macroscopic scale, the value of $\omega_e\tau_e$ indicates the relative importance of the Hall field and the Hall current. Hall effects are important when the Hall parameter, which is the ratio between the electron-cyclotron frequency and the electron-atom-collision frequency, is high. This happens when the magnetic field is strong or when the collision frequency is low. Hall currents are of great importance in many astrophysical problems, Hall accelerators, and flight MHD, as well as flows of plasma in a MHD power generator. Mazumder et al. [8] examined the Hall effects on combined free and forced convective hydromagnetic flow through a channel. Hall currents and surface temperature oscillation effects on natural convection MHD heat-generating flow were considered by Takhar and Ram [9]. Gourla and Katoch [10] presented the unsteady free convection MHD flow between heated vertical plates. Borkakati and Chakrabarty [11] studied the unsteady free convection MHD flow between two heated vertical parallel plates in an induced magnetic field. Jha [12] studied the unsteady MHD natural convective Couette flow. Singh and Pathak [13] studied the effect of rotation and Hall currents on mixed convection MHD flow through a porous medium filled in a vertical channel in the presence of thermal radiation. Das et al. [14] investigated the radiation effects on free convective MHD Couette flow started exponentially with variable wall temperature in the presence of heat generation. Effects of radiation on transient natural convection flow between two vertical walls were discussed by Mandal et al. [15]. Recently, Sarkar et al. [16] studied the effects of radiation on MHD free convective Couette flow in a rotating system. Seth and Ghosh [17] presented the unsteady hydromagnetic flow in a rotating channel in the presence of an inclined magnetic field. Pop et al. [18] examined the effects of the Hall current on free and forced convection flows in a rotating channel in the presence of an inclined magnetic field. Kalita and Lahkar [19] examined the effects of a magnetic field on unsteady free convection MHD flow between two heated vertical plates.

In the present paper, we have studied the combined effects of Hall currents and radiation on a hydromagnetic free convective flow of a viscous incompressible electrically conducting fluid in the presence of an inclined applied magnetic field. The temperature of the fluid motion is assumed to be changing with time. The magnetic Reynolds number is assumed to be small enough so that the induced magnetic field can be neglected. It is also assumed that there is no applied voltage, which implies the absence of an electrical field. The analytical solutions for velocity field, temperature distribution, shear stresses, and the rate of heat transfer at the channel plates are obtained and are presented graphically. In space technology and in nuclear engineering applications, such a problem is quite common. However, in these fields, the presence of a strong magnetic field and Hall

current taking effect plays an important role. In this paper, we investigate the solution in which the buoyancy, radiation, and Hall currents act simultaneously.

2. Formulation of the problem and its solution

Consider the unsteady hydromagnetic free convective flow of a viscous incompressible electrically conducting fluid between two infinite vertical parallel plates separated by a distance $2h$. The channel plates are electrically nonconducting. Choose a Cartesian coordinate system with the x-axis taken at the middle of the channel along the vertically upward direction, the z-axis normal to the plates, and the y-axis perpendicular to the xz-plane (Figure 1). Initially, at time $t \leq 0$, both the plates and the fluid are assumed to be at the same temperature, T_h. At time $t > 0$, the plate at $z = -h$ is heated with the temperature $T_h + (T_0 - T_h)(1 - e^{-nt})$, T_0 is the temperature at the plates at $z = h$ respectively, and $n(> 0)$, a real number, denotes the decay factor. The plate at $z = h$ is thermally insulated. A uniform magnetic field of strength B_0 is imposed at angle φ to the x-axis. It is also assumed that the radiative heat flux in the x-direction is negligible in comparison with that in the z-direction. As the plates are infinitely long along x and y directions, the velocity and temperature fields are functions of z and t only. In accordance with the Boussinesq approximation, we assume that all fluid properties are constant, except the density, which varies with temperature only in the body force term.

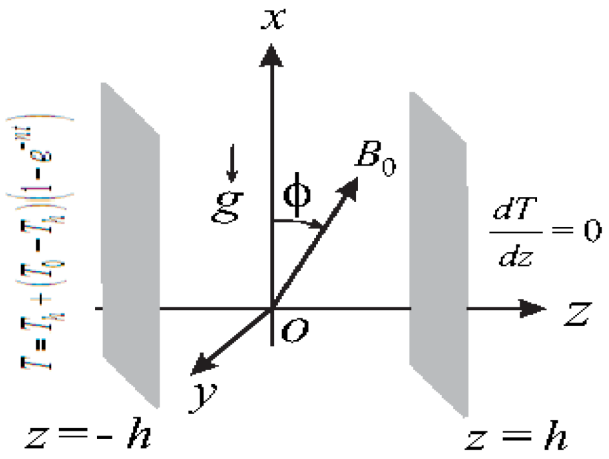

Figure 1. Geometry of the problem.

The Navier–Stokes MHD momentum equations under the Boussinesq approximation for the transient MHD channel flow with inclined magnetic field can be written in component form as:

$$\frac{\partial u}{\partial t} = \nu \frac{\partial^2 u}{\partial z^2} + g\beta(T - T_h) + \frac{B_0}{\rho} j_y \cos\varphi, \tag{1}$$

$$\frac{\partial v}{\partial t} = \nu \frac{\partial^2 v}{\partial z^2} - \frac{B_0}{\rho} j_x \cos\varphi, \tag{2}$$

where u and v are the velocity components, ν is the kinematic viscosity, ρ is the fluid density, and g is the acceleration due to gravity.

The energy equation is:

$$\rho c_p \frac{\partial T}{\partial t} = k \frac{\partial^2 T}{\partial z^2} - \frac{\partial q_r}{\partial z}, \tag{3}$$

where T is the temperature of the fluid, β is the coefficient of thermal expansion, ρ is the fluid density, k is the thermal conductivity, c_p is the specific heat at constant pressure, and q_r is the radiative heat flux. The effect of viscous and Joule dissipation is assumed to be negligible in the energy equation as small velocity is usually encountered in free convection flows.

The initial and boundary conditions for the velocity and temperature distributions are:

$$u = 0 = v, \;\; T = T_h \;\; \text{for} \;\; -h \le z \le h \;\; \text{and} \;\; t \le 0,$$

$$\begin{aligned} u = 0 = v, \;\; T = T_h + (T_0 - T_h)\,(1 - e^{-n\,t}) \;\; \text{at} \;\; z = -h \;\; \text{for} \;\; t > 0, \\ u = 0 = v, \;\; \frac{dT}{dz} = 0 \;\; \text{at} \;\; z = h \;\; \text{for} \;\; t > 0. \end{aligned} \tag{4}$$

The generalized Ohm law on taking Hall currents into account is [20]:

$$\vec{j} + \frac{\omega_e\,\tau_e}{B_0}\left(\vec{j} \times \vec{B}\right) = \sigma\left(\vec{E} + \vec{q} \times \vec{B}\right), \tag{5}$$

where $\vec{q}$, $\vec{B}$, $\vec{E}$, $\vec{j}$, σ, ω_e, and τ_e are respectively the velocity vector, the magnetic field vector, the electric field vector, the current density vector, the electric conductivity, the cyclotron frequency, and the electron collision time.

It is assumed that the magnetic Reynolds number Re_m for the flow is small so that the induced magnetic field can be neglected. This assumption is justified since the magnetic Reynolds number is generally very small for partially ionized gases. Thus, it can be assumed that due to the low magnetic Reynolds number the applied magnetic field is unaffected by the effect of the motion of the conducting fluid, i.e. the applied magnetic field will guide the flow, whereas the effect of the magnetic field on the fluid motion manifests itself in the form $\frac{\omega_e\,\tau_e}{B_0}\left(\vec{j} \times \vec{B}\right)$, which is known as the Lorentz force. The Lorentz force will be a linear function of velocity when $Re_m = 1$. If the strength of the magnetic field is high, then one cannot neglect the Hall current. This is a rather important case for some practical engineering problems. The electron-atom collision frequency is assumed to be relatively high, so that the Hall effects cannot be neglected [7].

The equation of continuity $\nabla \cdot \vec{q} = 0$ with no-slip condition at the plate gives $w = 0$ everywhere in the flow where $\vec{q} \equiv (u, v, w)$; u, v, and w are respectively the velocity components along the coordinate axes. The solenoidal relation $\nabla \cdot \vec{B} = 0$ gives B_z=constant $= B_0$ everywhere in the flow where $\vec{B} \equiv (0, 0, B_z)$. The conservation of electric current $\nabla \cdot \vec{j} = 0$ yields $j_z =$ constant where $\vec{j} \equiv (j_x, j_y, j_z)$. This constant is zero since $j_z = 0$ at the plates, which are electrically nonconducting. Hence, $j_z = 0$ everywhere in the flow. As the induced magnetic field is neglected, the Maxwell equation $\nabla \times \vec{E} = -\frac{\partial \vec{B}}{\partial t}$ becomes $\nabla \times \vec{E} = 0$, which gives $\frac{\partial E_x}{\partial z} = 0$ and $\frac{\partial E_y}{\partial z} = 0$ where $\vec{E} \equiv (E_x, E_y, E_z)$. This implies that $E_x =$ constant and $E_y =$ constant everywhere in the flow. Since there is no electrical field applied in the current regime under consideration, the polarization voltage is neglected. Therefore, it follows that $E_x = 0$ and $E_y = 0$, as indicated by Meyer [21].

In view of the above assumption, Eq. (5) yields:

$$j_x + m\,j_y \cos\varphi = \sigma\,v\,B_0 \cos\varphi, \tag{6}$$

$$j_y - m\,j_x \cos\varphi = -\sigma\,u\,B_0 \cos\varphi, \tag{7}$$

where $m = \omega_e \tau_e$ is the Hall parameter, which can take positive or negative values. Positive values of m mean that B_0 is upward. For negative values of m, B_0 is downward.

Solving for j_x and j_y from Eqs. (6) and (7), we have

$$j_x = \frac{\sigma B_0 \cos\varphi}{1 + m^2 \cos^2\varphi} \left(v + mu\cos\varphi\right), \tag{8}$$

$$j_y = \frac{\sigma B_0 \cos\varphi}{1 + m^2 \cos^2\varphi} \left(mv\cos\varphi - u\right), \tag{9}$$

where $m = \omega_e \tau_e$ is the Hall parameter.

On the use of Eqs. (8) and (9), the fluid flow be governed by the following system of equations:

$$\frac{\partial u}{\partial t} = \nu \frac{\partial^2 u}{\partial z^2} + g\beta(T - T_h) + \frac{\sigma B_0^2 \cos\varphi}{1 + m^2 \cos^2\varphi} \left(mv\cos\varphi - u\right), \tag{10}$$

$$\frac{\partial v}{\partial t} = \nu \frac{\partial^2 v}{\partial z^2} - \frac{\sigma B_0^2 \cos\varphi}{1 + m^2 \cos^2\varphi} \left(v + mu\cos\varphi\right). \tag{11}$$

It was shown by Cogley et al. [22] that in the optically thin limit for a nongray gas near equilibrium, the following relation holds:

$$\frac{\partial q_r}{\partial y} = 4(T - T_h) \int_0^\infty K_{\lambda_h^*} \left(\frac{\partial e_{\lambda^* p}}{\partial T}\right)_h d\lambda^*, \tag{12}$$

where K_λ^* is the absorption coefficient, λ^* is the wave length, $e_{\lambda^* p}$ is the Planck function, and subscript h indicates that all quantities have been evaluated at temperature T_h, which is the temperature of the wall at time $t \leq 0$. Thus, our study is limited to the small difference of plate temperature from the fluid temperature. Greif et al. [23] showed that for an optically thin limit, the fluid does not absorb its own emitted radiation; this means that there is no self-absorption, but the fluid does absorb radiation emitted by the boundaries. Treatments to the radiative heating are either in the limit where photon mean free paths are very small, called optically thick, or very long, called optically thin. At high temperatures the presence of thermal radiation alters the distribution of temperature in the boundary layer, which in turn affects the heat transfer at the channel walls.

On the use of Eq. (12), Eq. (3) becomes

$$\rho c_p \frac{\partial T}{\partial t} = k \frac{\partial^2 T}{\partial y^2} - 4\left(T - T_h\right) I, \tag{13}$$

where

$$I = \int_0^\infty K_{\lambda_h^*} \left(\frac{\partial e_{\lambda^* p}}{\partial T}\right)_h d\lambda^*. \tag{14}$$

Introducing nondimensional variables

$$\eta = \frac{z}{h}, \quad \tau = \frac{\nu t}{h^2}, \quad (u_1, v_1) = \frac{h}{\nu}(u, v), \quad \theta = \frac{T - T_h}{T_0 - T_h}, \tag{15}$$

Eqs. (10), (11), and (13) become

$$\frac{\partial u_1}{\partial \tau} = \frac{\partial^2 u_1}{\partial \eta^2} + Gr\,\theta + \frac{M^2 \cos\varphi}{1 + m^2 \cos^2\varphi}\left(m v_1 \cos\varphi - u_1\right), \tag{16}$$

$$\frac{\partial v_1}{\partial \tau} = \frac{\partial^2 v_1}{\partial \eta^2} - \frac{M^2 \cos\varphi}{1 + m^2 \cos^2\varphi}\left(v_1 + m u_1 \cos\varphi\right), \tag{17}$$

$$Pr\,\frac{\partial \theta}{\partial \tau} = \frac{\partial^2 \theta}{\partial \eta^2} - R\theta, \tag{18}$$

where $M^2 = \frac{\sigma B_0^2 h^2}{\rho \nu}$ is the magnetic parameter that represents the ratio of the magnetic field strength to the viscous force, $R = \frac{4Ih^2}{k}$ is the radiation parameter, $Gr = \frac{g\beta(T_0 - T_h)h^3}{\nu^2}$ is the Grashof number that approximates the ratio of the buoyancy force to the viscous force acting on a fluid, and $Pr = \frac{\rho \nu c_p}{k}$ is the Prandtl number, which measures the ratio of momentum diffusivity to thermal diffusivity.

The corresponding initial and boundary conditions for u_1, v_1, and θ are

$$u_1 = 0 = v_1,\ \theta = 0 \ \text{ for } \ -1 \le \eta \le 1 \ \text{ and } \ \tau \le 0,$$

$$u_1 = 0 = v_1,\ \ \theta = 1 - e^{-\omega\tau} \ \text{ at } \ \eta = -1 \ \text{ for } \ \tau > 0, \tag{19}$$

$$u_1 = 0 = v_1,\ \ \frac{d\theta}{d\eta} = 0 \ \text{ at } \ \eta = 1 \ \text{ for } \ \tau > 0,$$

where $\omega = \frac{n h^2}{\nu}$ is the temperature frequency parameter.

Combining Eqs. (16) and (17), we get

$$\frac{\partial F}{\partial \tau} = \frac{\partial^2 F}{\partial \eta^2} + Gr\,\theta - a F, \tag{20}$$

where

$$F = u_1 + i v_1,\ \ a = \frac{M^2 \cos^2\varphi}{1 + m^2 \cos^2\varphi}(1 - im\cos\varphi) \ \text{ and } \ i = \sqrt{-1}. \tag{21}$$

The corresponding boundary conditions for F and θ are

$$F = 0,\ \theta = 0 \ \text{ for } \ -1 \le \eta \le 1 \ \text{ and } \ \tau \le 0,$$

$$F = 0,\ \ \theta = 1 - e^{-\omega\tau} \ \text{ at } \ \eta = -1 \ \text{ for } \ \tau > 0, \tag{22}$$

$$F = 0,\ \ \frac{d\theta}{d\eta} = 0 \ \text{ at } \ \eta = 1 \ \text{ for } \ \tau > 0.$$

The Laplace transform method solves differential equations and corresponding initial and boundary value problems. The Laplace transform has the advantage that it solves problems directly, initial value problems without determining first a general solution, and nonhomogeneous differential equations without solving first

the corresponding homogeneous equations. In order to obtain the exact solution of the present problem, we will use the Laplace transform technique. On the use of the Laplace transformation, Eqs. (20) and (18) become

$$s\,\bar{F} = \frac{d^2\bar{F}}{d\eta^2} + Gr\,\bar{\theta} - a\,\bar{F}, \tag{23}$$

$$Pr\,s\,\bar{\theta} = \frac{d^2\bar{\theta}}{d\eta^2} - R\bar{\theta}, \tag{24}$$

where

$$\bar{F}(\eta,s) = \int_0^\infty F(\eta,\tau)\,e^{-s\tau}\,d\tau \;\text{ and }\; \bar{\theta}(\eta,s) = \int_0^\infty \theta(\eta,\tau)\,e^{-s\tau}\,d\tau. \tag{25}$$

The corresponding boundary conditions for $\bar{F}$ and $\bar{\theta}$ are

$$\bar{F}(-1,s) = 0,\;\; \bar{\theta}(-1,s) = \frac{1}{s} - \frac{1}{s+\omega},$$

$$\bar{F}(1,s) = 0,\;\; \frac{d\bar{\theta}}{d\eta}(1,s) = 0. \tag{26}$$

Solution of Eqs. (23) and (24) subject to the boundary conditions of Eq. (26) are given by

$$\bar{\theta}(\eta,s) = \frac{\omega}{s(s+\omega)}\,\frac{\cosh\sqrt{s\,Pr+R}\,(1-\eta)}{\cosh 2\sqrt{s\,Pr+R}}, \tag{27}$$

$$\bar{F}(\eta,s) = \begin{cases} \dfrac{\omega\,Gr}{(1-Pr)\,s\,(s+\omega)\,(s+b)}\left[\dfrac{\cosh\sqrt{s\,Pr+R}(1-\eta)}{\cosh 2\sqrt{s\,Pr+R}}\right. \\ \left. -\frac{\sinh\sqrt{s+a}(1-\eta)}{\sinh 2\sqrt{s+a}} - \frac{\sinh\sqrt{s+a}\,(1+\eta)}{\sinh 2\sqrt{s+a}\cosh 2\sqrt{s\,Pr+R}}\right] & \text{for } Pr \neq 1 \\ \dfrac{\omega\,Gr}{(a-R)\,s\,(s+\omega)}\left[\dfrac{\cosh\sqrt{s+R}(1-\eta)}{\cosh 2\sqrt{s+R}}\right. \\ \left. -\frac{\sinh\sqrt{s+a}(1-\eta)}{\sinh 2\sqrt{s+a}} - \frac{\sinh\sqrt{s+a}\,(1+\eta)}{\sinh 2\sqrt{s+a}\cosh 2\sqrt{s+R}}\right] & \text{for } Pr = 1, \end{cases} \tag{28}$$

where $b = \frac{a-R}{1-Pr}$.

The inverse Laplace transforms of Eqs. (27) and (28) give the solution for the temperature and the velocity distributions respectively as

$$\begin{aligned} \theta(\eta,\tau) \;\; &= \;\; \frac{\cosh\sqrt{R}(1-\eta)}{\cosh 2\sqrt{R}} - \frac{\cosh\sqrt{R-\omega\,Pr}\,(1-\eta)}{\cosh 2\sqrt{R-\omega\,Pr}}\,e^{-\omega\,\tau} \\ &\quad + \sum_{k=0}^{\infty} \frac{\pi(2k+1)\,(-1)^k\,e^{s_1\tau}}{4s_1(s_1+\omega)\,Pr}\,\cos(2k+1)\frac{\pi}{4}(1-\eta), \end{aligned} \tag{29}$$

$$F(\eta,\tau)=\begin{cases}
\dfrac{Gr}{(1-Pr)}\left[\dfrac{1}{b}\left\{\dfrac{\cosh\sqrt{R}(1-\eta)}{\cosh 2\sqrt{R}}-\dfrac{\sinh\sqrt{a}(1-\eta)}{\sinh 2\sqrt{a}}-\dfrac{\sinh\sqrt{a}(1+\eta)}{\sinh 2\sqrt{a}\cosh 2\sqrt{R}}\right\}\right.\\
-\dfrac{e^{-\omega\tau}}{b-\omega}\left\{\dfrac{\cosh\sqrt{R-\omega\,Pr}(1-\eta)}{\cosh 2\sqrt{R-\omega\,Pr}}-\dfrac{\sinh\sqrt{a-\omega}(1-\eta)}{\sinh 2\sqrt{a-\omega}}\right.\\
\left.\left.-\dfrac{\sinh\sqrt{a}(1+\eta)}{\sinh 2\sqrt{a-\omega}\cosh 2\sqrt{R-\omega\,Pr}}\right\}\right.\\
+\sum_{k=0}^{\infty}\frac{(2k+1)\,\pi\,e^{s_1\tau}}{4s_1(s_1+\omega)(s_1+b)\,Pr}\\
\times(-1)^k\left\{\cos(2k+1)\frac{\pi}{4}(1-\eta)-\frac{\sinh\sqrt{s_1+a}(1-\eta)}{\sinh 2\sqrt{s_1+a}}\right\}\\
\left.+\sum_{k=0}^{\infty}\dfrac{\pi\,k\,e^{s_2\tau}}{2s_2(s_2+\omega)(s_2+b)}(-1)^k\left\{\sin\dfrac{k\pi}{2}(1-\eta)+\dfrac{\sinh\frac{k\pi}{2}(1+\eta)}{\cosh 2\sqrt{s_2Pr+R}}\right\}\right]\text{for}\;\; Pr\neq 1\\
\dfrac{Gr}{(a-R)}\left[\left\{\dfrac{\cosh\sqrt{R}(1-\eta)}{\cosh 2\sqrt{R}}-\dfrac{\sinh\sqrt{a}(1-\eta)}{\sinh 2\sqrt{a}}-\dfrac{\sinh\sqrt{a}(1+\eta)}{\sinh 2\sqrt{a}\cosh 2\sqrt{R}}\right\}\right.\\
-e^{-\omega\tau}\left\{\dfrac{\cosh\sqrt{R-\omega}(1-\eta)}{\cosh 2\sqrt{R-\omega}}-\dfrac{\sinh\sqrt{a-\omega}(1-\eta)}{\sinh 2\sqrt{a-\omega}}\right.\\
\left.\left.-\dfrac{\sinh\sqrt{a}(1+\eta)}{\sinh 2\sqrt{a-\omega}\cosh 2\sqrt{R-\omega}}\right\}\right.\\
+\sum_{k=0}^{\infty}\dfrac{(2k+1)\,\pi\,e^{s_3\tau}}{4s_3(s_3+\omega)}(-1)^k\left\{\cos(2k+1)\dfrac{\pi}{4}(1-\eta)-\dfrac{\sinh\sqrt{s_3+a}(1-\eta)}{\sinh 2\sqrt{s_3+a}}\right\}\\
\left.+\sum_{k=0}^{\infty}\dfrac{\pi\,k\,e^{s_2\tau}}{2s_2(s_2+\omega)(s_2+b)}(-1)^k\left\{\sin\dfrac{k\pi}{2}(1-\eta)+\dfrac{\sinh\frac{k\pi}{2}(1+\eta)}{\cosh 2\sqrt{s_2+R}}\right\}\right]\text{for}\;\; Pr=1,
\end{cases}\tag{30}$$

where

$$s_1=-\frac{1}{Pr}\left[R+(2k+1)^2\frac{\pi^2}{16}\right],\quad s_2=-\left[a+\frac{k^2\pi^2}{4}\right],\quad s_3=-\left[R+(2k+1)^2\frac{\pi^2}{16}\right].\tag{31}$$

In the absence of Hall currents $(m=0)$, Eqs. (29) and (30) are reduced to that obtained by Kalita and Lahkar [19].

The steady-state solution for the temperature and the velocity distributions are respectively given by

$$\theta(\eta,\tau)=\frac{\cosh\sqrt{R}(1-\eta)}{\cosh 2\sqrt{R}},\tag{32}$$

$$F(\eta,\tau)=\begin{cases}
\frac{Gr}{(1-Pr)b}\left[\frac{\cosh\sqrt{R}(1-\eta)}{\cosh 2\sqrt{R}}-\frac{\sinh\sqrt{a}(1-\eta)}{\sinh 2\sqrt{a}}-\frac{\sinh\sqrt{a}(1+\eta)}{\sinh 2\sqrt{a}\cosh 2\sqrt{R}}\right] & \text{for}\;\; Pr\neq 1\\
\frac{Gr}{(a-R)}\left[\frac{\cosh\sqrt{R}(1-\eta)}{\cosh 2\sqrt{R}}-\frac{\sinh\sqrt{a}(1-\eta)}{\sinh 2\sqrt{a}}-\frac{\sinh\sqrt{a}(1+\eta)}{\sinh 2\sqrt{a}\cosh 2\sqrt{R}}\right] & \text{for}\;\; Pr=1,
\end{cases}\tag{33}$$

3. Results and discussion

We have presented the nondimensional velocity and temperature distributions for several values of magnetic parameter M^2, Hall parameter m, radiation parameter R, Grashof number Gr, Prandtl number Pr, magnetic

field inclination φ, frequency parameter ω, and angular frequency $\omega\tau$ in Figures 2–13. It is seen from Figure 2 that both the primary velocity u_1 and the secondary velocity v_1 decrease with an increase in magnetic parameter

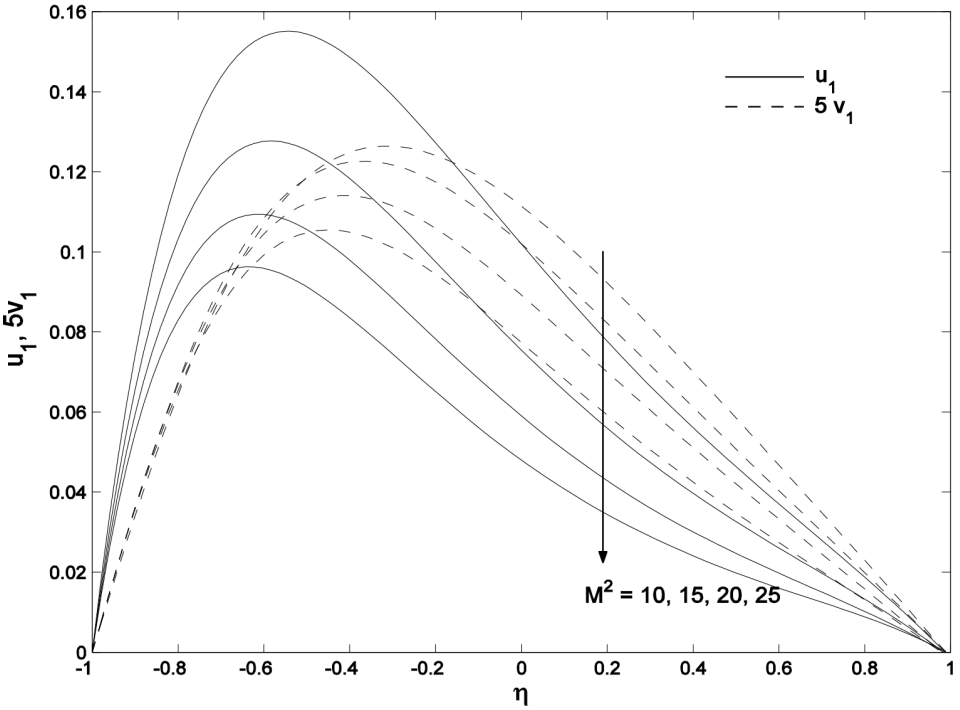

Figure 2. Primary and second velocities for M^2 when $m = 0.5$, $Gr = 5$, $\omega = 2$, $R = 2$, $Pr = 0.025$, $\tau = 0.5$, $\omega\tau = \frac{\pi}{2}$, and $\varphi = \frac{\pi}{4}$.

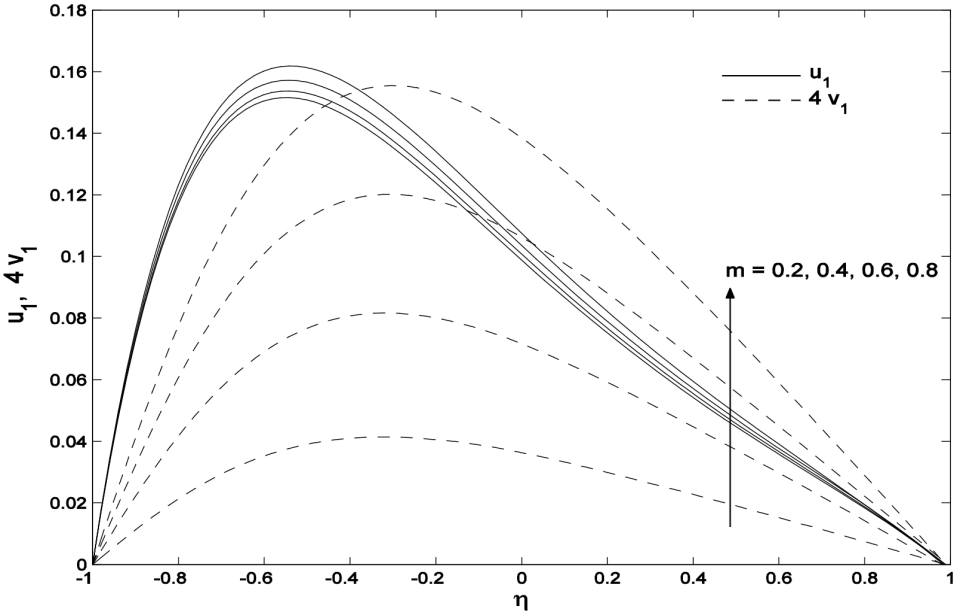

Figure 3. Primary and second velocities for m when $M^2 = 10$, $Gr = 5$, $\omega = 2$, $R = 2$, $Pr = 0.025$, $\tau = 0.5$, $\omega\tau = \frac{\pi}{2}$, and $\varphi = \frac{\pi}{4}$.

M^2. This is because the presence of a magnetic field in an electrically conducting fluid introduces a Lorentz force (a resistive force similar to the drag force), which acts against the flow. This resistive force tends to slow down the fluid flow and hence the fluid velocity components decrease with an increase in magnetic parameter. This trend is consistent with many classical studies on magnetoconvection flow. Figure 3 reveals that both

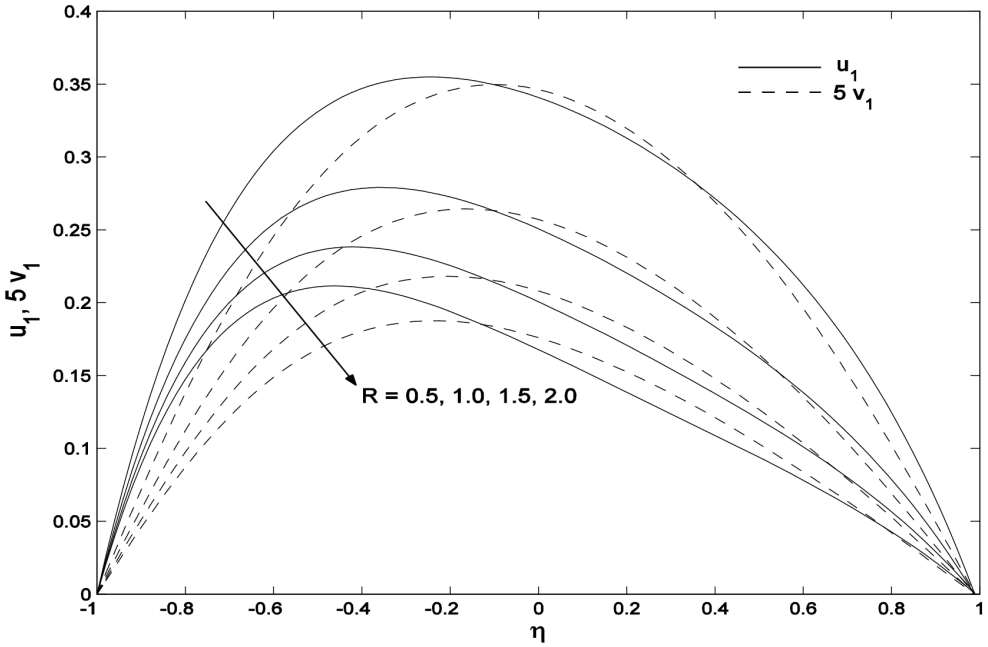

Figure 4. Primary and second velocities for R when $M^2 = 10$, $Gr = 5$, $\omega = 2$, $m = 0.5$, $Pr = 0.025$, $\tau = 0.5$, $\omega\tau = \frac{\pi}{2}$, and $\varphi = \frac{\pi}{4}$.

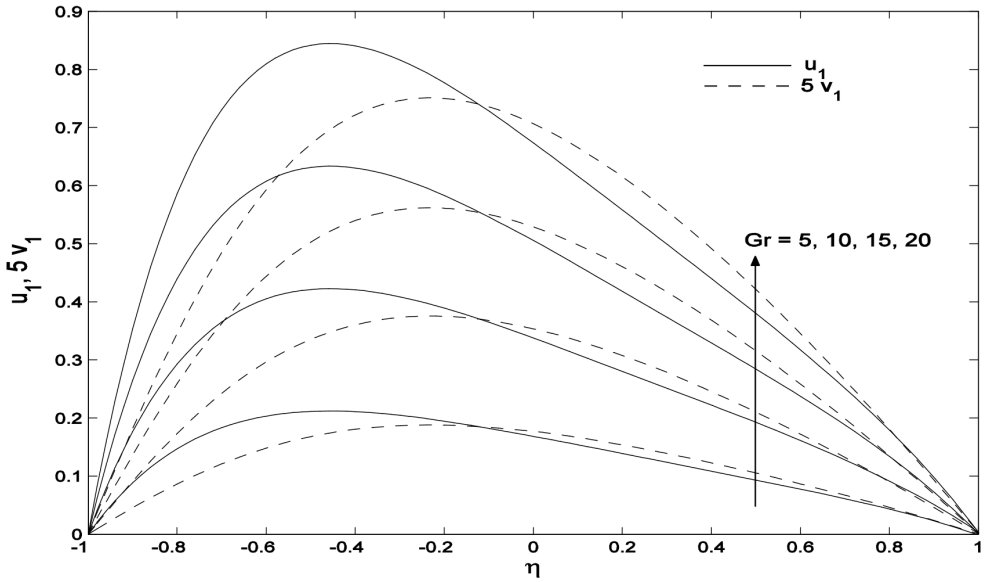

Figure 5. Primary and second velocities for Gr when $M^2 = 10$, $R = 2$, $\omega = 2$, $m = 0.5$, $Pr = 0.025$, $\tau = 0.5$, $\omega\tau = \frac{\pi}{2}$, and $\varphi = \frac{\pi}{4}$.

the primary velocity u_1 and the secondary velocity v_1 increase with an increase in Hall parameter m. Since the magnetic field is strong, the electromagnetic force becomes very large, which results in the phenomenon of the Hall currents. The Hall currents cause an increase in the secondary velocity. The secondary velocity is totally dependent on the Hall currents. Thus, the secondary velocity can be manipulated by increasing or decreasing the Hall parameter. The Hall parameter m has a marked effect on the velocity profiles. It is observed

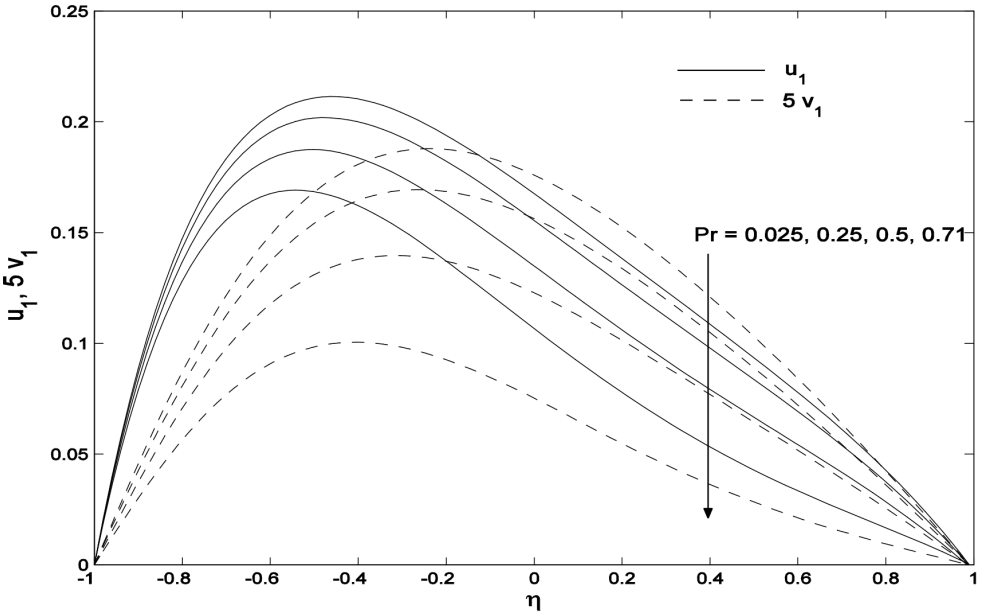

Figure 6. Primary and second velocities for Pr when $M^2 = 10$, $Gr = 5$, $\omega = 2$, $m = 0.5$, $R = 2$, $\tau = 0.5$, $\omega\tau = \frac{\pi}{2}$, and $\varphi = \frac{\pi}{4}$.

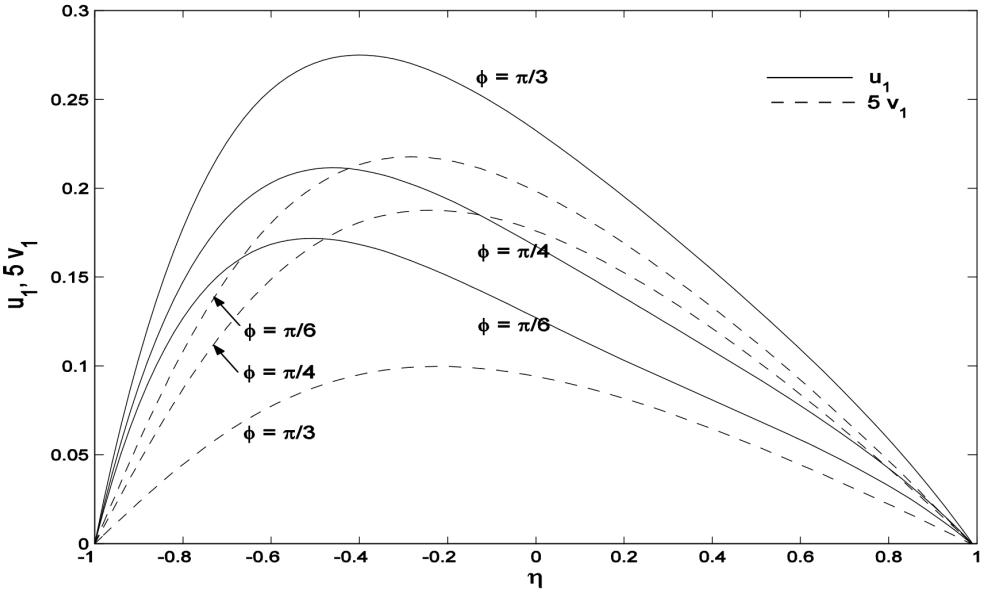

Figure 7. Primary and second velocities for φ when $M^2 = 10$, $Gr = 5$, $\omega = 2$, $m = 0.5$, $Pr = 0.025$, $\tau = 0.5$, $\omega\tau = \frac{\pi}{2}$, and $R = 2$.

that an increasing value of m increases the velocity profiles until they reach the hydrodynamic values. This is because the effective conductivity $\frac{\sigma \cos\varphi}{1+m^2\cos^2\varphi}$ decreases as m increases for the fixed value of φ. Since the fluid is assumed to be weakly ionized, we can consider the value of the Hall parameter m less than unity [7]. It is seen from Figure 4 that an increase in radiation parameter R leads to a decrease in the primary velocity u_1 and the secondary velocity v_1. The radiation parameter arises only in the energy equation in the thermal diffusion

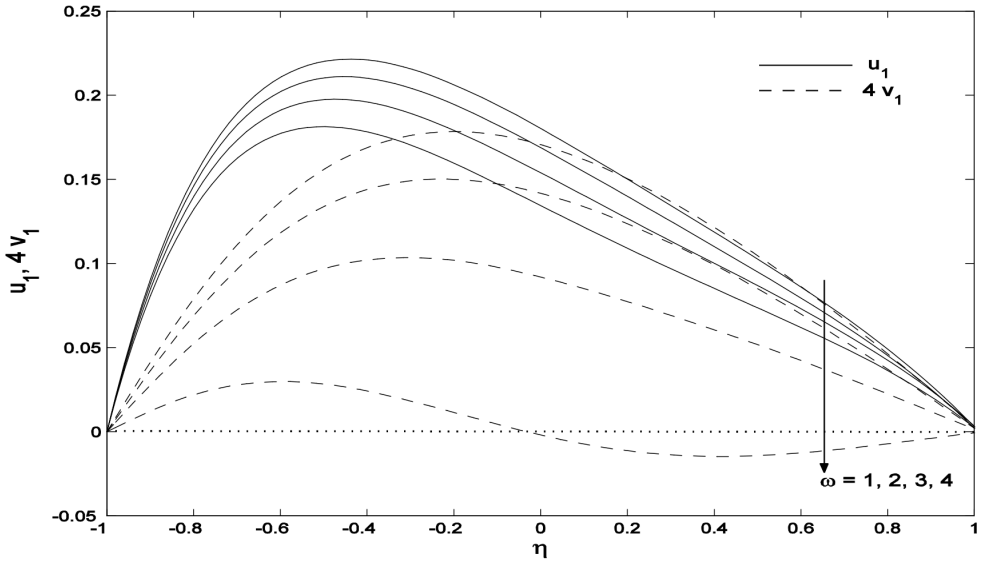

Figure 8. Primary and second velocities for ω when $M^2 = 10,\ Gr = 5,\ R = 2,\ m = 0.5,\ Pr = 0.025,\ \tau = 0.5,$ $\omega\tau = \frac{\pi}{2}$, and $\varphi = \frac{\pi}{4}$.

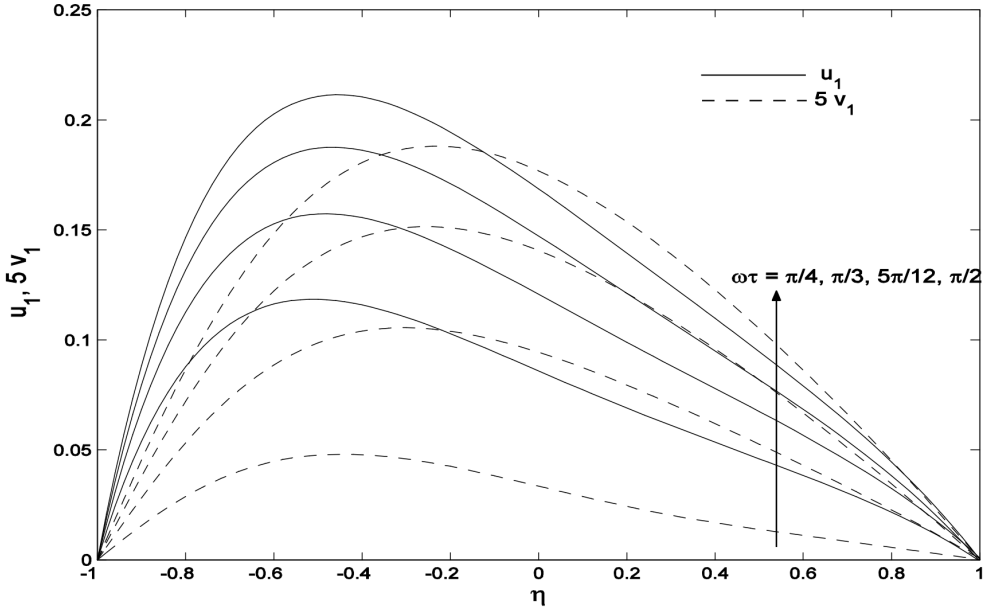

Figure 9. Primary and second velocities for $\omega\tau$ when $M^2 = 10,\ Gr = 5,\ \omega = 2,\ m = 0.5,\ Pr = 0.025,\ \tau = 0.5,$ $R = 2$, and $\varphi = \frac{\pi}{4}$.

term, and via coupling of the temperature field with the buoyancy terms in the momentum equation, the fluid velocity is indirectly influenced by thermal radiation effects. An increase in the radiation parameter implies less interaction of radiation with the momentum boundary layer and hence the flow becomes decelerated. We focus on the positive values of the buoyancy parameter, i.e. Grashof number Gr, which corresponds to the cooling problem. The cooling problem is often encountered in engineering applications. Figure 5 reveals that both the primary velocity u_1 and the secondary velocity v_1 increase with an increase in Grashof number Gr.

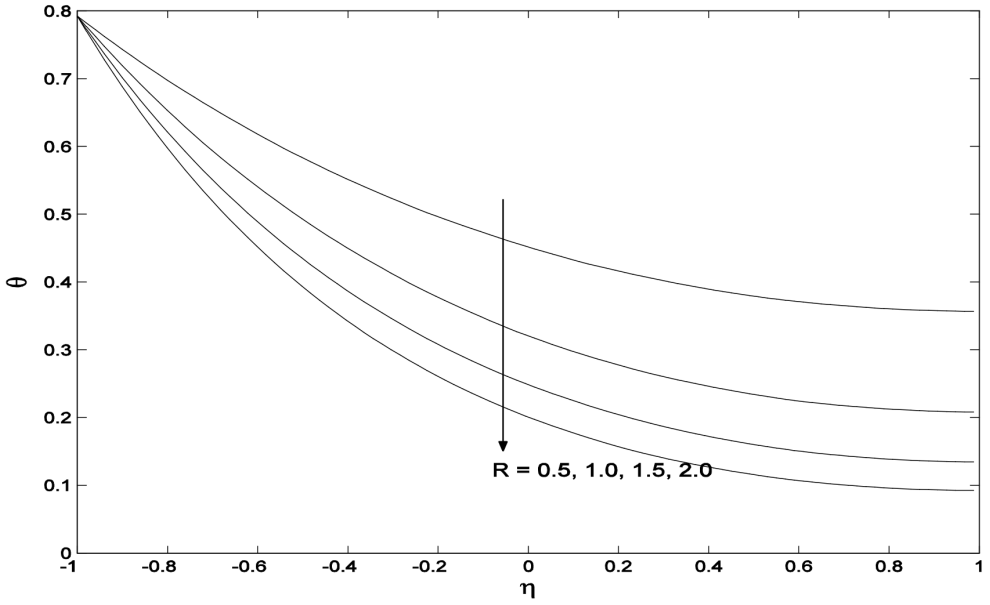

Figure 10. Temperature for R when $Pr = 0.025$, $\omega = 2$, and $\omega\tau = \frac{\pi}{2}$.

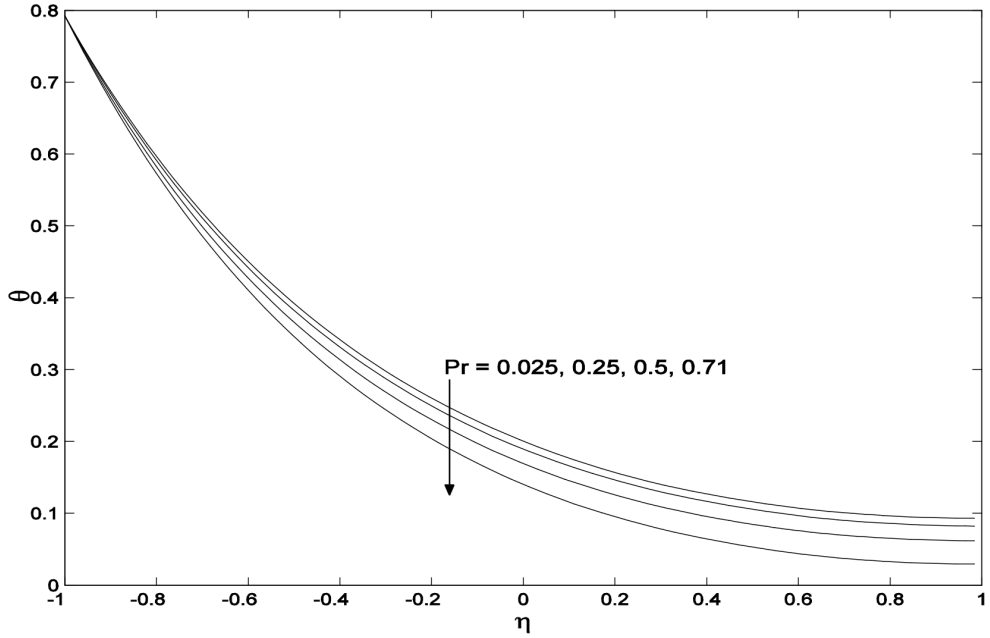

Figure 11. Temperature for Pr when $R = 2$, $\omega = 2$, and $\omega\tau = \frac{\pi}{2}$.

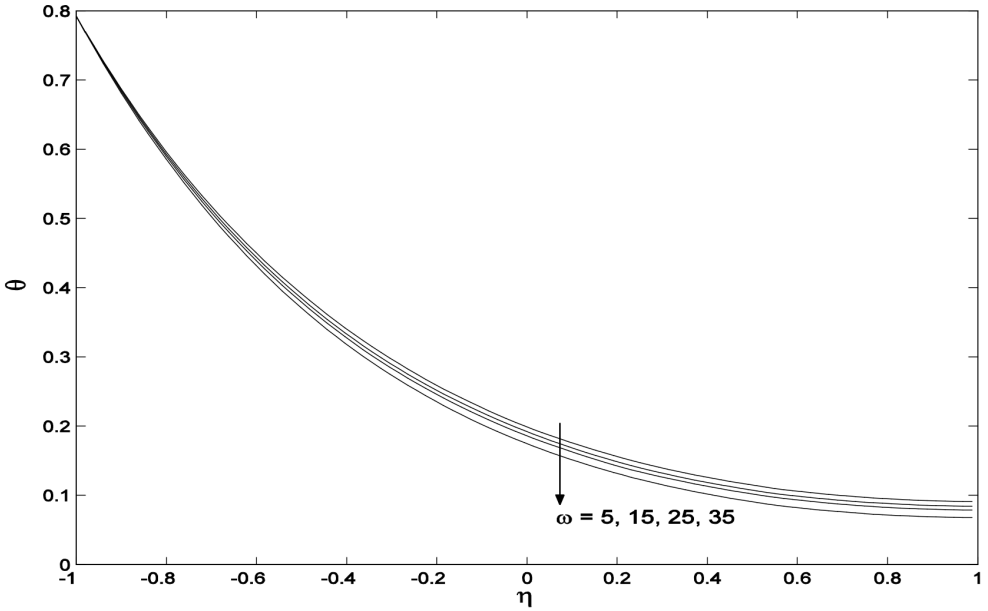

Figure 12. Temperature for ω when $Pr = 0.025$, $R = 2$, and $\omega\tau = \frac{\pi}{2}$.

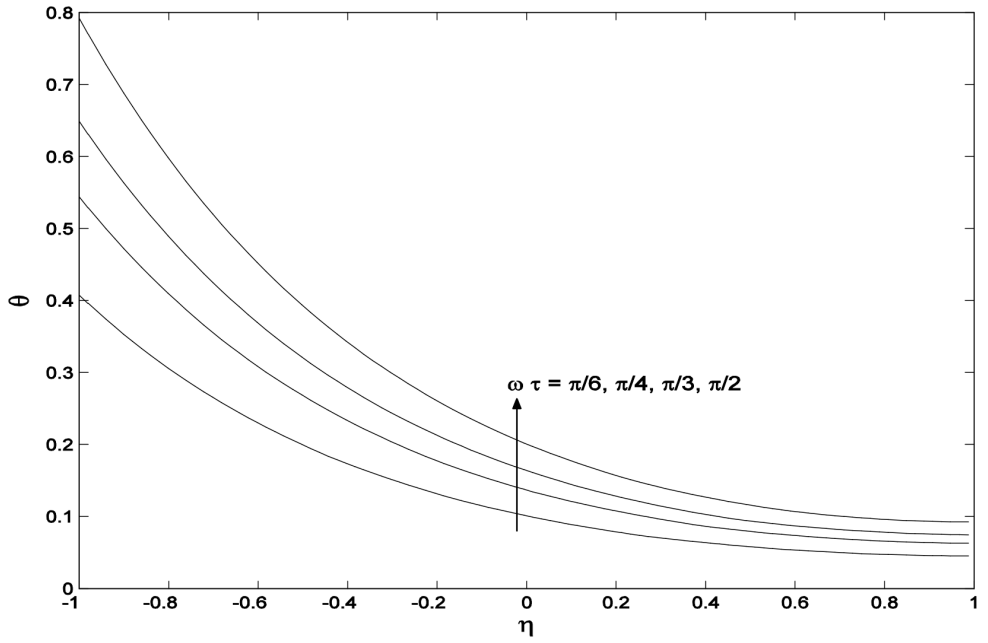

Figure 13. Temperature for R when $Pr = 0.025$, $\omega = 2$, and $R = 2$.

The Grashof number signifies the relative effect of the thermal buoyancy force on the viscous hydrodynamic force in the boundary layer. As expected, it is observed that there is a rise in the velocity components due to the enhancement of thermal buoyancy force. The maximum of the velocity profiles shifts toward the left half of the channel due to the greater buoyancy force in this part of the channel due to the presence of the hotter plate. In the left half there lies the hot plate at $\eta = -1$ and heat is transferred from the hot plate to the fluid, and consequently the buoyancy force enhances the flow velocity further. Figure 6 shows that both the primary

velocity u_1 and the secondary velocity v_1 decrease with an increase in Prandtl number Pr. Prandtl number Pr then provides a measure of relative effectiveness of momentum and energy transport of diffusion in the velocity and thermal boundary layers respectively, e.g., in the case of gases Pr is nearly equal to unity and therefore energy and momentum transfer by diffusion are comparable, whereas for liquid metals $Pr < 1$ and the energy diffusion rate greatly exceeds the momentum diffusion rate. On the other hand, in the case of oils, $Pr > 1$. From this interpretation it implies that the value of Pr influences the growth of the velocity and the thermal boundary layer. Thus, the Prandtl number acts as the conducting link between the velocity field and the temperature field since it involves momentum transfer that consequently yields heat transfer. Physically, this is true because the increase in the Prandtl number is due to increase in the viscosity of the fluid, which makes the fluid thick and hence causes a decrease in the velocity of the fluid. It is worth mentioning that the present investigation deals with those functional fluids that act as liquid metals in many engineering applications because of their ability to reduce the temperature of the system. For instance, liquid metals are used in nuclear power plants and mercury, sodium, alloys, lead-bismuth, and bismuth are extensively utilized as coolants. It is seen from Figure 7 that the primary velocity u_1 is accelerated whereas the secondary velocity v_1 is retarded with an increase in magnetic field inclination φ. As magnetic field inclination φ increases, the hydromagnetic drag force decreases. Consistent with this, it is observed that a rise in inclination clearly accelerates the primary flow and decelerates the secondary flow. Figure 8 demonstrates that both the primary velocity u_1 and the secondary velocity v_1 decrease with an increase in frequency parameter ω. The frequency of surface temperature oscillations exerts a marked influence on the primary velocity u_1 and the secondary velocity v_1, as shown in Figure 8, which are decreased substantially with a rise in ω. Back flow is therefore augmented with increasing oscillation frequency, with the maximum effect at close proximity to the plate $\eta = -1$. It is revealed from Figure 9 that both the primary velocity u_1 and the secondary velocity v_1 increase with an increase in angular frequency $\omega\tau$. The oscillations near the middle of the channel are of great significance.

The effects of radiation parameter R, Prandtl number Pr, frequency parameter ω, and angular frequency $\omega\tau$ on the temperature distribution are shown in Figures 10–13. It is observed from Figures 10–12 that the fluid temperature θ decreases with an increase in radiation parameter R, Prandtl number Pr, or frequency parameter ω. This result qualitatively agrees with the expectations, since the effect of radiation decreases the rate of energy transport to the fluid, thereby decreasing the temperature of the fluid. Prandtl number Pr is the ratio of the viscosity to the thermal diffusivity. An increase in thermal diffusivity leads to a decrease in Prandtl number. Therefore, thermal diffusion has a tendency to reduce the fluid temperature. It is revealed in Figure 13 that an increase in angular frequency $\omega\tau$ leads to a rise in fluid temperature θ.

The rate of heat transfer $\theta'(-1,\tau)$ $\left(= \frac{\partial\theta}{\partial\eta}\Big|_{\eta=-1}\right)$ and temperature $\theta(1,\tau)$ at the plate $\eta = 1$ are respectively given by

$$\theta'(-1,\tau) = -\sqrt{R}\tanh 2\sqrt{R} + \sqrt{R-\omega Pr}\tanh 2\sqrt{R-\omega Pr}\, e^{-\omega\tau} + \sum_{k=0}^{\infty}\frac{(2k+1)^2\pi^2 e^{s_1\tau}}{16\, s_1(s_1+\omega)\, Pr}, \tag{34}$$

$$\theta(1,\tau) = sech 2\sqrt{R} - e^{-\omega\tau} sech 2\sqrt{R-\omega Pr} + \sum_{k=0}^{\infty}\frac{\pi(2k+1)(-1)^k e^{s_1\tau}}{4 s_1(s_1+\omega)\, Pr}, \tag{35}$$

where s_1 is given by Eq. (29).

Numerical results of the rate of heat transfer $-\theta'(-1,\tau)$ at the plate $\eta = -1$ for several values of radiation parameter R, Prandtl number Pr, frequency parameter ω, and angular frequency $\omega\tau$ are presented

in Table 1. Table 1 shows that the rate of heat transfer $-\theta^{'}(-1,\tau)$ increases with an increase in radiation parameter R, Prandtl number Pr, frequency parameter ω, or angular frequency $\omega\tau$. This can be attributed to the fact that as thermal radiation increases, the dominance effect of temperature gradient increases, leading to an increase in the rate of heat transfer. This may be also explained by the fact that frictional forces become dominant with increasing values of Prandtl number Pr and hence yield a greater heat transfer rate. An increase in Prandtl number reduces the thermal boundary layer thickness. The Prandtl number signifies the ratio of momentum diffusivity to thermal diffusivity. Fluids with lower Prandtl numbers will possess higher thermal conductivities so that heat can diffuse from the sheet faster than for higher Pr fluids (thinner boundary layers). Hence, the Prandtl number can be used to increase the rate of cooling in conducting flows. It is clear that the rate of heat transfer is higher in the presence of thermal radiation. The negative value of $\theta^{'}(-1,\tau)$ physically explains that there is heat flow from the hot plate $\eta=-1$ to the fluid. It is observed from Table 2 that the plate temperature $\theta(1,\tau)$ at $\eta=1$ decreases with an increase in radiation parameter R, Prandtl number Pr, or frequency parameter ω. Furthermore, it is seen from Table 2 that the plate temperature $\theta(1,\tau)$ at $\eta=1$ increases with an increase in angular frequency $\omega\tau$.

The nondimensional shear stresses at the plate $\eta=1$ are obtained as follows:

$$\tau_{x_1}+i\tau_{y_1}=\left(\frac{\partial F}{\partial \eta}\right)_{\eta=1}=\begin{cases}\frac{Gr}{(1-Pr)}\left[\frac{\sqrt{a}}{b}\operatorname{cosech2}\sqrt{a}\left(1-\cosh 2\sqrt{a}\,\operatorname{sech2}\sqrt{R}\right)\right.\\ -\dfrac{e^{-\omega\tau}}{b-\omega}\sqrt{a-\omega}\,\operatorname{cosech2}\sqrt{a-\omega}\\ \times\left(1-\cosh 2\sqrt{a-\omega}\,\operatorname{sech2}\sqrt{R-\omega Pr}\right)\\ -\displaystyle\sum_{k=0}^{\infty}\frac{(2k+1)(-1)^k\pi e^{s_1\tau}}{4s_1(s_1+\omega)(s_1+b)Pr}\sqrt{s_1+a}\coth\sqrt{s_1+a}\\ \left.-\displaystyle\sum_{k=0}^{\infty}\frac{\pi k(-1)^k e^{s_2\tau}}{2s_2(s_2+\omega)(s_2+b)}\left\{1-(-1)^k\operatorname{sech2}\sqrt{s_2Pr+R}\right\}\right] & \text{for}\quad Pr\neq 1\\ \frac{Gr}{(a-R)}\left[\frac{\sqrt{a}}{b}\operatorname{cosech2}\sqrt{a}\left(1-\cosh 2\sqrt{a}\,\operatorname{sech2}\sqrt{R}\right)\right.\\ -\dfrac{e^{-\omega\tau}}{b-\omega}\sqrt{a-\omega}\,\operatorname{cosech2}\sqrt{a-\omega}\\ \times\left(1-\cosh 2\sqrt{a-\omega}\,\operatorname{sech2}\sqrt{R-\omega}\right)\\ -\displaystyle\sum_{k=0}^{\infty}\frac{(2k+1)(-1)^k\pi e^{s_3\tau}}{4s_3(s_3+\omega)}\sqrt{s_3+a}\coth\sqrt{s_3+a}\\ \left.-\displaystyle\sum_{k=0}^{\infty}\frac{\pi k(-1)^k e^{s_2\tau}}{2s_2(s_2+\omega)}\left\{1-(-1)^k\operatorname{sech2}\sqrt{s_2+R}\right\}\right] & \text{for}\quad Pr=1,\end{cases}\tag{36}$$

where s_1, s_2, and s_3 are given by Eq. (29).

Numerical results of the nondimensional shear stresses at the plate $\eta=1$ are presented in Figures 14–19 for several values of Hall parameter m, radiation parameter R, Grashof number Gr, inclination of magnetic φ, frequency parameter ω, and angular frequency $\omega\tau$ when $Pr=0.025$. Figure 14 shows that the absolute values of the shear stress τ_{x_1} due to the primary flow and the shear stress τ_{y_1} due to the secondary flow at the plate $\eta=1$ reduce with an increase in either radiation parameter R or magnetic parameter M^2. Since

Table 1. Rate of heat transfer $-\theta^{'}(-1,\tau)$ at the plate $\eta=-1$.

	Pr			ω			$\omega\tau$		
R	0.015	0.020	0.025	2	3	4	$\pi/6$	$\pi/4$	$\pi/3$
0.5	0.50292	0.50474	0.50657	0.50657	0.51127	0.51611	0.28164	0.36146	0.42290
1.0	0.76710	0.76828	0.76946	0.76946	0.77245	0.77549	0.40958	0.53729	0.63558
1.5	0.95850	0.95941	0.96032	0.96032	0.96262	0.96495	0.50475	0.66641	0.79084
2.0	1.11471	1.11548	1.11625	1.11625	1.11818	1.12013	0.58333	0.77244	0.91800

Table 2. Temperature $\theta(1,\tau)$ at the plate $\eta=1$.

	Pr			ω			$\omega\tau$		
R	0.015	0.020	0.025	2	3	4	$\pi/6$	$\pi/4$	$\pi/3$
0.5	0.35996	0.35867	0.35736	0.35736	0.35397	0.35040	0.16919	0.23597	0.32692
1.0	0.20892	0.20836	0.20779	0.20779	0.20633	0.20482	0.10048	0.13856	0.19043
1.5	0.13489	0.13460	0.13429	0.13429	0.13352	0.13273	0.06566	0.09002	0.12319
2.0	0.09279	0.09261	0.09243	0.09243	0.09198	0.09151	0.04551	0.06216	0.08484

the intense amount of the magnetic field literally increases the Lorentz force that significantly opposes the flow in the reverse direction, the magnetic field thus acts as the retarding force that causes the shear stresses to decrease significantly. It is observed from Figures 15–18 that the absolute values of the shear stresses τ_{x_1} and τ_{y_1} increase with an increase in Hall parameter m, Grashof number Gr, inclination of magnetic field φ, or angular frequency $\omega\tau$. This happens because the electrical conductivity of the fluid decreases with increasing m, which ultimately reduces the magnetic damping force and hence the shear stresses are increased considerably. The absolute values of the shear stresses at the channel wall $\eta=1$ enhance with increasing buoyancy force due to increase in flow velocity. An increase in frequency of plate temperature oscillations ω also reduces the components of shear stress at the plate $\eta=1$ as shown in Figure 19.

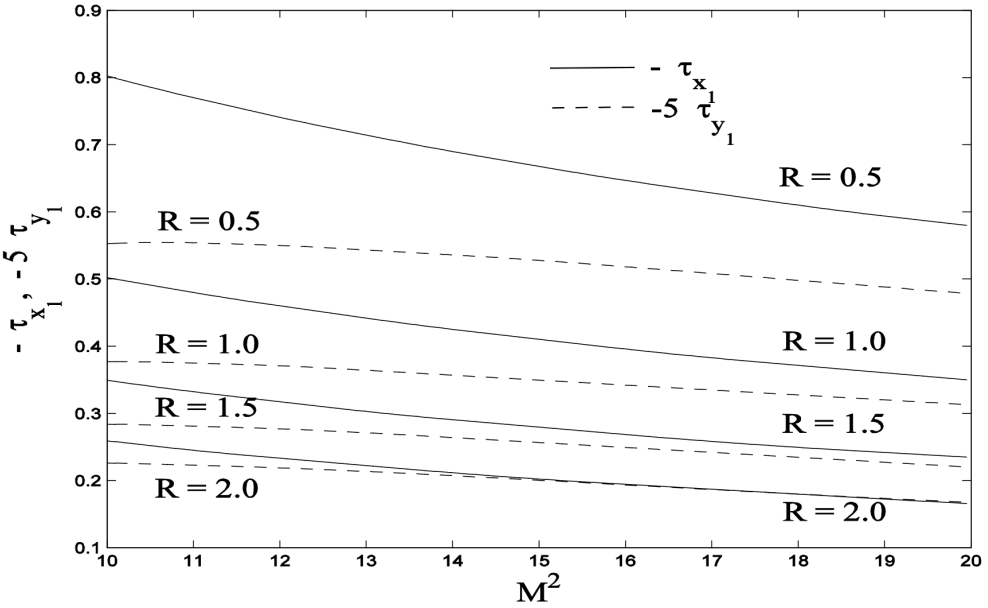

Figure 14. Shear stresses τ_{x_1} and τ_{y_1} for R when $m=0.5$, $Gr=5$, $\omega=2$, $\tau=0.5$, $\omega\tau=\frac{\pi}{2}$, and $\varphi=\frac{\pi}{4}$.

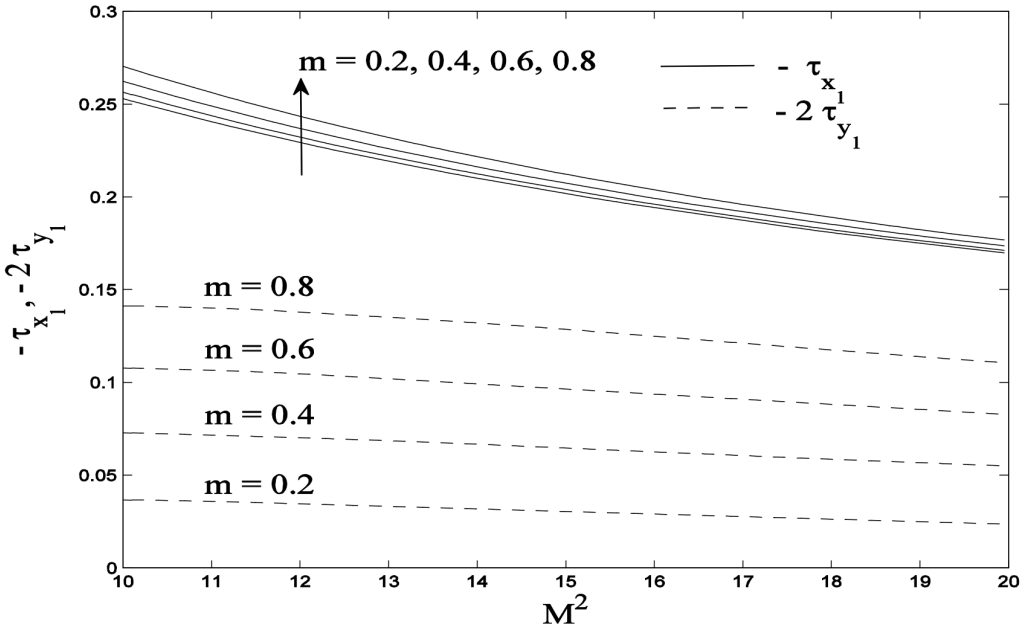

Figure 15. Shear stresses τ_{x_1} and τ_{y_1} for m when $R = 2$, $Gr = 5$, $\omega = 2$, $\tau = 0.5$, $\omega\tau = \frac{\pi}{2}$, and $\varphi = \frac{\pi}{4}$.

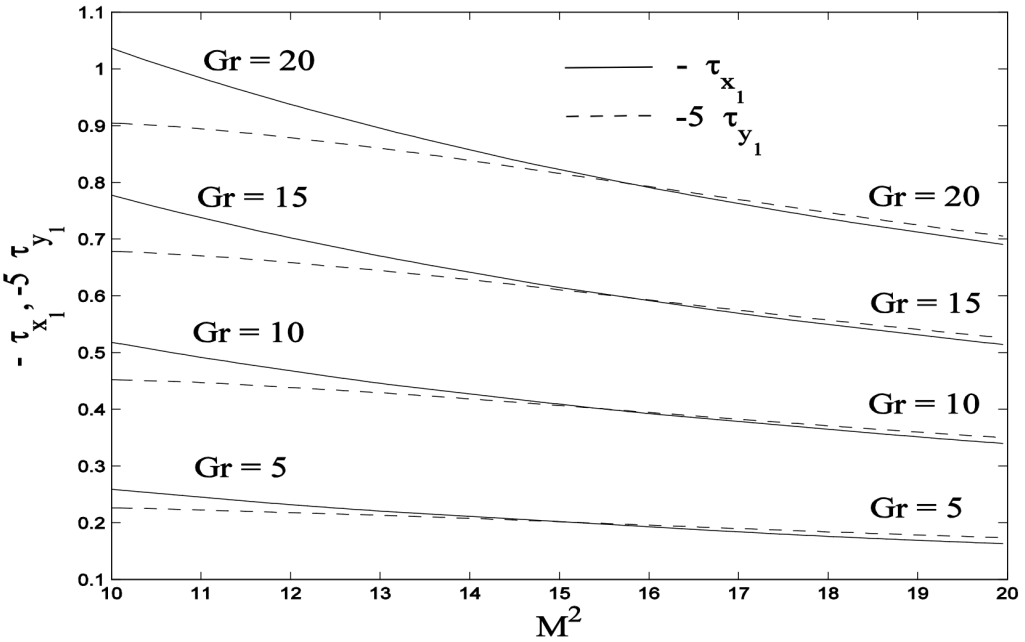

Figure 16. Shear stresses τ_{x_1} and τ_{y_1} for Gr when $R = 2$, $Gr = 5$, $\omega = 2$, $\tau = 0.5$, $\omega\tau = \frac{\pi}{2}$, and $\varphi = \frac{\pi}{4}$.

4. Conclusion

Analytical solutions have been obtained for the transient MHD free convection flow in a heated vertical parallel plate channel in the presence of an inclined magnetic field taking Hall currents into account. The effects of pertinent parameters on the flow field, the temperature distribution, and the shear stresses have been discussed. Introducing the Hall terms causes an increase in the secondary velocity component and affects the primary velocity component. Magnetic field and radiation have a retarding influence on the primary velocity. An

increase in magnetic field inclination leads to acceleration of the primary velocity while suppressing the secondary velocity. The preset model finds applications in hybrid MHD energy generators and also magnetic materials processing systems.

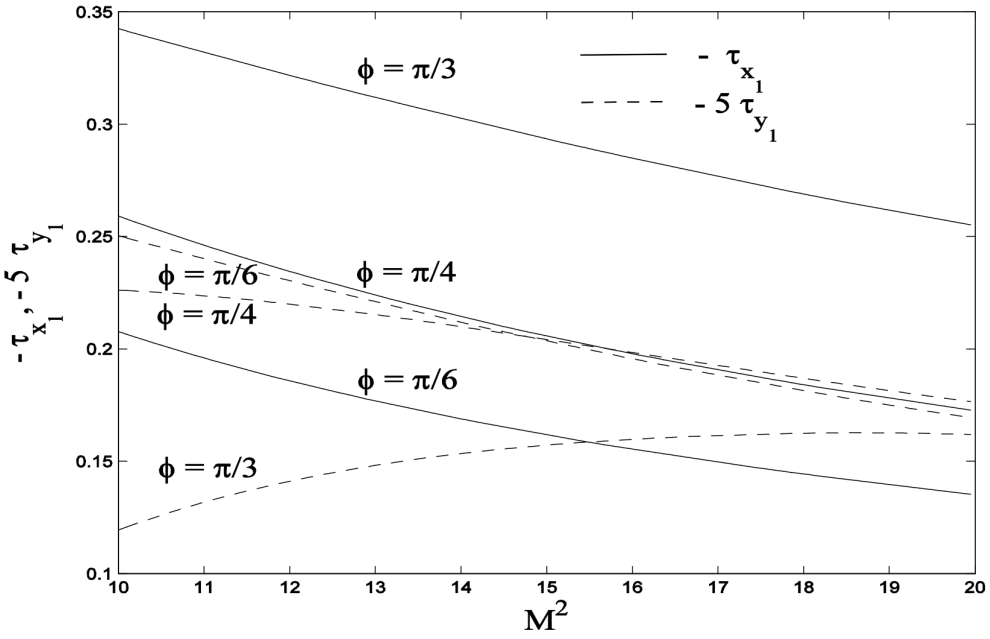

Figure 17. Shear stresses τ_{x_1} and τ_{y_1} for φ when $R = 2,\ Gr = 5,\ \omega = 2,\ \tau = 0.5$, and $\omega\tau = \frac{\pi}{2}$.

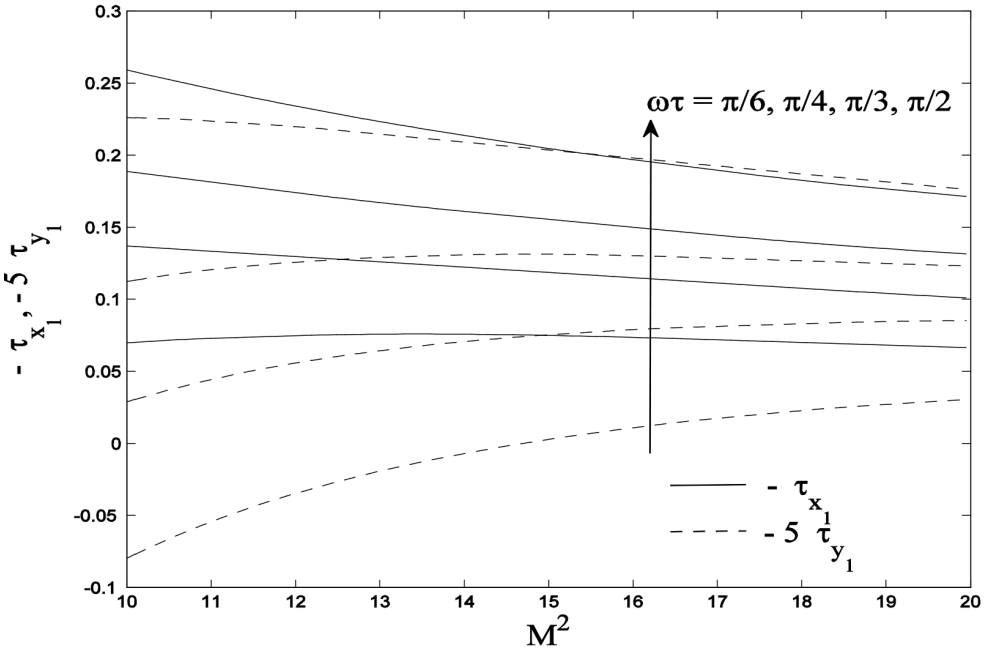

Figure 18. Shear stresses τ_{x_1} and τ_{y_1} for $\omega\tau$ when $R = 2,\ Gr = 5,\ \tau = 0.5,\ \omega = 2$, and $\varphi = \frac{\pi}{4}$.

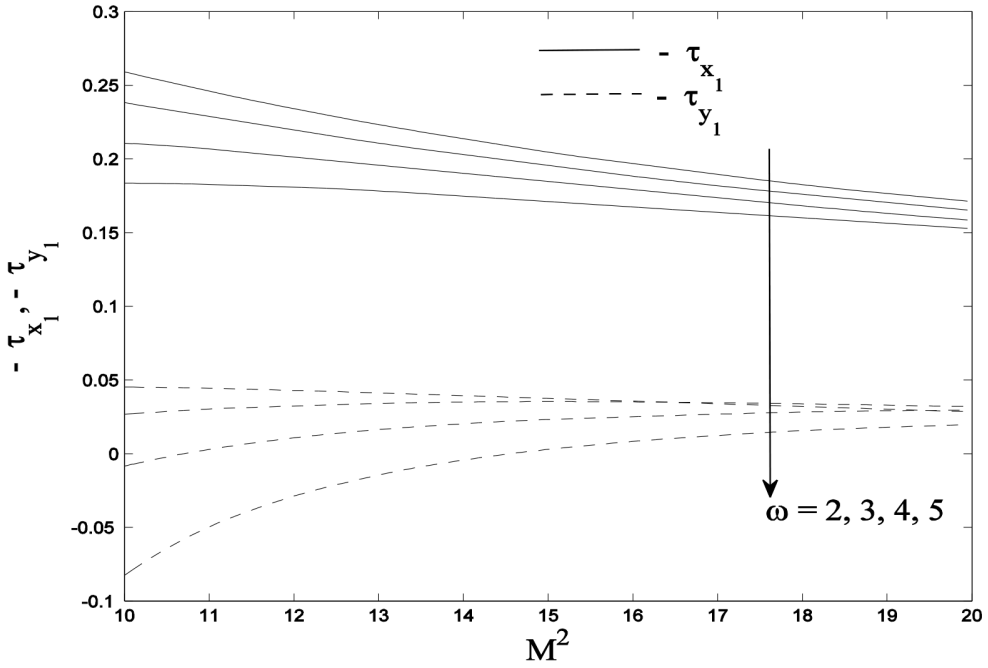

Figure 19. Shear stresses τ_{x_1} and τ_{y_1} for ω when $R = 2$, $Gr = 5$, $\tau = 0.5$, $\omega\tau = \frac{\pi}{2}$, and $\varphi = \frac{\pi}{4}$.

References

[1] Takenouchi K. Transient magnetohydrodynamic channel flow with axial symmetry at a supersonic speed. J Phys Soc Jpn 1985; 54: 1329–1338.

[2] Hardianto T, Sakamoto N, Harada N. Computational study of diagonal channel magnetohydrodynamic power generation. Int J Energy Techn Policy 2008; 6: 96–111.

[3] Narasimhan MN. Transient Magnetohydrodynamic Flow in an Annular Channel, Technical Report. Madison, WI, USA: University of Wisconsin-Madison Mathematics Research Center; 1963.

[4] Takhar HS, Ram PC. Free convection in hydromagnetic flows of a viscous heat-generating fluid with wall temperature oscillation and Hall currents. Astrophys Space Sci 1991; 183: 193–198.

[5] Ryabinin AG, Khozhainov AI. Exact and approximate formulations of problems for unsteady flows of conducting fluids in MHD channels. Fluid Dyn 1967; 2: 107–109 .

[6] Barmin AA, Uspenskii VS. Development of pulsation regimes in one-dimensional unsteady MHD flows with switching off of the electrical conductivity. Fluid Dyn 1986; 21: 18–30.

[7] Sutton G, Sherman A. Engineering Magnetohydrodynamics. New York, NY, USA: McGraw-Hill; 1965.

[8] Mazumder BS, Gupta AS, Datta N. Hall effects on combined free and forced convective hydromagnetic flow through a channel. Int J Heat Mass Tran 1976; 14: 285–292.

[9] Takhar HS, Ram PC. Free convection in hydromagnetic flows of a viscous heat-generating fluid with wall temperature oscillation and Hall currents. Astrophys Space Sci 1991; 183: 193–198.

[10] Gourla MG, Katoch S. Unsteady free convection MHD flow between heated vertical plates. Ganita 1991; 42: 143–154.

[11] Borkakati AK, Chakrabarty S. Unsteady free convection MHD flow between two heated vertical parallel plates in induced magnetic field. Indian J Theor Phys 1999; 47: 43–60.

[12] Jha BK. Natural convection in unsteady MHD Couette flow. Heat Mass Transfer 2001; 37: 329–331.

[13] Singh KD, Pathak R. Effect of rotation and Hall current on mixed convection MHD flow through a porous medium filled in a vertical channel in presence of thermal radiation. Indian J Pure Ap Phy 2012; 50: 77–85.

[14] Das S, Sarkar BC, Jana RN. Radiation effects on free convection MHD Couette flow started exponentially with variable wall temperature in presence of heat generation. Open Journal of Fluid Dynamics 2012; 2: 14–27.

[15] Mandal C, Das S, Jana RN. Effect of radiation on transient natural convection flow between two vertical walls. International Journal of Applied Information Systems 2012; 2: 49–56.

[16] Sarkar BC, Das S, Jana RN. Effects of radiation on MHD free convective Couette flow in a rotating system. International Journal of Engineering Research and Applications 2012; 2: 2346–2359.

[17] Seth GS, Ghosh SK. Unsteady hydromagnetic flow in a rotating channel in the presence of inclined magnetic field. Int J Eng Sci 1986; 24: 1183–1193.

[18] Pop I, Ghosh SK, Nandi DK. Effects of the Hall current on free and forced convection flows in a rotating channel in the presence of an inclined magnetic field. Magnetohydrodynamics 2001; 37: 348–359.

[19] Kalita B, Lahkar J. Magnetic field effects on unsteady free convection MHD flow between two heated vertical plates (one adiabatic). Advanced Studies in Theoretical Physics 2012; 6: 765–775.

[20] Cowling TG. Magnetohydrodynamics. New York, NY, USA: Interscience; 1957.

[21] Meyer RC. On reducing aerodynamic heat transfer rates by magnetohydrodynamic techniques. J Aerospace Sci 1958; 25: 561–566.

[22] Cogley AC, Vincentine WC, Gilles SE. A differential approximation for radiative transfer in a nongrey gas near equilibrium. AIAA J 1968; 6: 551–555.

[23] Grief R, Habib IS, Lin JC. Laminar convection of a radiating gas in a vertical channel. J Fluid Mech 1970; 46: 513–520.